Conformation of the N-Terminal Segment of a Monocysteine Mutant of Troponin I from Cardiac Muscle†

Wen-Ji Dong,‡ Murali Chandra,§ Jun Xing,‡ R. John Solaro,§ and Herbert C. Cheung*,‡

Department of Biochemistry and Molecular Genetics, University of Alabama at Birmingham, Birmingham, Alabama 35294-2041, and Department of Physiology and Biophysics, College of Medicine, University of Illinois at Chicago, Chicago, Illinois 60612

Received September 3, 1996; Revised Manuscript Received April 3, 1997⊗

ABSTRACT: A monocysteine mutant of cardiac muscle troponin I, cTnI(S5C/C81I/C98S), was generated from a mouse cTnI cDNA clone and expressed in a bacterial system. Cys-5 was modified with the fluorescent sulfhydryl reagent IAANS to probe the conformation of the N-terminal extension of the mutant and the mutant complexed with cardiac muscle troponin C. Our emphasis was on the effect of phosphorylation of Ser-23 and Ser-24 by protein kinase A on the conformation of the N-terminal segment. Phosphorylation resulted in an 8-nm red-shift of the emission spectrum of the attached IAANS probe and a reduction of its quantum yield by a factor of 4−5. The intensity decay of nonphosphorylated IAANS-labeled mutant was complex and had to be described by a sum of three exponential terms, with lifetimes in the range 0.1−5 ns. A fourth component in the range 7−9 ns was required to describe the intensity decay of the phosphorylated mutant. Phosphorylation also reduced the weighted mean lifetime, consistent with the changes observed in the steady-state fluorescence parameters and a 33% decrease in the global rotational correlation time calculated from anisotropy decay data. This change in correlation time suggested a decrease in the axial ratio of the protein. The fluorescence changes of the labeled mutant induced by phosphorylation were carried over to its complex with troponin C. The Stern−Volmer plots of acrylamide quenching of the steady-state fluorescence were essentially linear for nonphosphorylated mutant but displayed pronounced concave downward curvatures for the phosphorylated protein under all conditions studied. The present results are interpreted in terms of a more compact hydrodynamic shape of the phosphorylated cTnI mutant and are consistent with a folded conformation of the N-terminal extension induced by phosphorylation of the two serines. These conformational changes may play a role in the modulation of cardiac muscle contractility by troponin I phosphorylation.

Activation of vertebrate striated muscle is triggered by calcium binding to troponin, which is located on the thin filament. Troponin consists of three nonidentical subunits: troponin C (TnC),[1] which is the calcium-binding component, TnI, which is the inhibitory subunit of actomyosin ATPase, and TnT, which binds to tropomyosin. Primarily on the basis of information derived from studies of fast skeletal muscle TnI and TnC (Zot & Potter, 1987; Tao et al., 1990), calcium binding to the regulatory sites of TnC is believed to strengthen the interaction of TnC with TnI, and concomitantly to weaken the inhibitory TnI with actin. With these changes tropomyosin moves toward the groove of the double-helical actin filament. These events "switch" on the thin filament, leading to release of ATP hydrolysis products from the myosin active site. Activation of muscle thus involves calcium-dependent partial dissociation of TnI from actin and release of tropomyosin from its inhibitory state.

Although the isoforms of TnI from cardiac and fast skeletal muscle are highly similar in their amino acid sequences, unique structural features of cTnI suggest that there may be important differences in the way cTnI functions in cardiac myofilaments. The cardiac isoform contains an additional 32-residue N-terminal extension in which are located two adjacent serine residues at positions 23 and 24. The importance of this additional N-terminal segment was recognized when it was reported that these two serines can be phosphorylated by protein kinase A (Moir et al., 1980; Swiderek et al., 1988). It was shown in an earlier study that the extent of cTnI phosphorylation correlated with the degree of positive inotropy in rabbit heart stimulated by catecholamines (Solaro et al., 1976). Several lines of evidence indicate that phosphorylation of cTnI may have an important regulatory role in controlling cardiac function (Solaro, 1986). The calcium affinity of the single regulatory site of cTnC in reconstituted cardiac troponin was reduced when cTnI was phosphorylated by PKA (Robertson et al., 1982). Recent studies have shown that the N-terminal segment of cTnI regulates myofibrillar ATPase activity only when the segment is phosphorylated (Guo et al., 1994; Wattanapermool et al., 1995). The mechanism by which cTnI phosphorylation affects the calcium affinity of cTnC and regulates myofibrillar ATPase activity remains obscure. A reasonable hypothesis is that the mechanism may involve

† This work was supported by NIH Grants HL52508 (H.C.C.) and HL49934 (R.J.S.), and Postdoctoral Fellowships from the Muscular Dystrophy Association to W.-J.D. and from the American Heart Association of Metropolitan Chicago to M.C.

* Corresponding author: (205) 934-2485. FAX: (205) 975-4621. E-mail: hccheung@bmg.bhs.uab.edu.

‡ University of Alabama at Birmingham.

§ University of Illinois at Chicago.

⊗ Abstract published in *Advance ACS Abstracts,* May 15, 1997.

[1] Abbreviations: TnI, troponin I; TnC, troponin C; cTnI, troponin I from cardiac muscle; cTnC, troponin C from cardiac muscle; PCR, polymerase chain reaction; IAANS, 2-[(4′-iodoacetamido)anilino]-naphthalene-6-sulfonic acid; DTT, dithiothreitol; EGTA, ethylene glycol bis(β-aminoethyl ether)-*N*,*N*,*N*′,*N*′-tetraacetic acid; MOPS, 3-(*N*-morpholino)propanesulfonic acid; PKA, protein kinase A.

S0006-2960(96)02226-X CCC: $14.00

a change in the interaction between cTnI and cTnC which is modulated by a new phosphorylation-induced conformation of the N-terminal extension. This induced conformation may have a more symmetric hydrodynamic shape (Liao et al., 1992).

The present study was initiated in an attempt to define the structural characteristics of the N-terminal segment of cTnI for understanding the role of phosphorylation in calcium regulation of cardiac function. To address this problem a mutant of cTnI, cTnI(S5C/C81I/C98S), was generated and labeled with the fluorescent probe IAANS at Cys-5. Large changes were observed in the steady-state and time-resolved fluorescence properties of this labeled mutant induced by phosphorylation by PKA. These results support the notion that phosphorylation induces large conformational changes in the N-terminal segment of cTnI.

MATERIALS AND METHODS

Preparation of TnC from Cardiac Muscle. Cardiac muscle troponin was extracted from an ether powder prepared from the left ventricle of fresh bovine hearts (Potter, 1982). TnC was separated from the other two troponin subunits on a CM-Sephadex C-50-120 column in the presence of 6 M urea, 50 mM Tris at pH 8.0, and 1 mM DTT. Crude cTnC was eluted from the same buffer and subsequently purified on a DEAE-Sephadex A-50 column in the same buffer and eluted with a gradient of 0−0.5 M KCl. The purity of the protein was monitored by sodium dodecyl sulfate polyacrylamide gel electrophoresis, and the purified protein was lyophilized in the presence of 0.1 M KCl, 0.5 mM EGTA, 0.5 mM DTT, and 20 mM imidazole at pH 7.2 and stored at −20 °C.

Preparation of Mutant cTnI. The methodology for performing mutagenesis by PCR was as described by Ho et al. (1989). The mutant cTnI(S5C/C81I/C98S) was generated in two steps.

(1) Isolation of S5C/C98S cTnI DNA Fragment. Two separate reactions were carried out using cTnI plasmid DNA (Guo et al., 1994) as the template DNA. The nucleotide sequence of the forward primer (primer 1: 5′GAGATATACCATGGCTGATGAATGCAGCGATGCGG3′) for reaction I was designed to include codons corresponding to amino acids 1−8 of cTnI (underlined) which also included a change in codon at position 5 to convert Ser to Cys. This sequence was flanked on the 5′ side by nucleotides of the pET3d vector (Novagen) including the *Nde*I restriction enzyme site. The nucleotide sequence of the reverse primer (primer 2: 5′AGCGTGAAGCTGTCG**GCT**TAAFTCCTGAAGCTC 3′) for reaction I contained codons for amino acids 93−103. The codon at position 98 was designed to substitute Cys with Ser. Nucleotide sequence of the forward primer (primer 3: 5′GAGCTTCAGGACTTAAGCCGAC**AGC**TTCACGCT3′) for reaction II was complimentary to primer 2. Nucleotide sequence of the reverse primer (primer 4: 5′CGTGTCTGGATCC**TCA**GCCCTCAAACTTTTTCTTG 3′) for reaction II corresponded to the noncoding strand of the cTnI gene which included codons for amino acids 206−211 (underlined). This was flanked on the 5′ side by a stop codon (in bold) and the *Bam*HI restriction enzyme site. The PCR products from these two separate reactions were gel purified and combined, and final PCR was carried out in the presence of primers 1 and 4. The final PCR product containing the full-length cTnI DNA fragment (S5C/C98S) was gel purified and used as the template DNA in the second step to generate S5C/*C*81I/*C*98*S* cTn*I* DNA Fragment.

(2) Isolation of S5C/C81I/C98S cTnI Fragment. Two separate PCR were carried out using S5C/C98S DNA fragment as the template and the following oligonucleotides as primers. The forward primer for reaction I was primer 1. The nucleotide sequence of the reverse primer (primer 5: 5′CAACTCCAAAGGCTG**GAT**ACGAGTCCTCAGAAC 3′) corresponded to the noncoding strand which included codons for amino acids 76−86. This sequence incorporated a change in codon at position 81 (in bold) to substitute Cys with Ile. The nucleotide sequence of the forward primer (primer 6: 5′ GTTCTGAGGACTCGT**ATC**CAGCCTTTGGAGTTG 3′) for reaction II was complementary to primer 5. The reverse primer for reaction II was primer 4. The PCR products from these two reactions were gel purified, digested with *Nco*I and *Bam*HI, and ligated into the pET3d expression vector (Novagen). Plasmid DNA from the clone carrying the mutant cTnI(C5S/C81I/C98S) was purified, and the gene was sequenced to ascertain the authenticity of the sequence. Expression and purification of cTnI were as described before (Guo et al., 1994).

Phosphorylation of Cardiac TnI Mutant. Mutant cTnI was phosphorylated at pH 7.0 in 50 mM KH_2PO_4, 0.5 mM EGTA, 0.5 mM DTT, 125 units of the catalytic subunit of protein kinase A/mg of cTnI. The reaction was started by adding ATP to a final concentration of 0.5 mM, followed by incubation at 30 °C for 20 min. The solution was then dialyzed exhaustively at 4 °C against a solution containing 30 mM MOPS at pH 7.0, 1 mM EGTA, 0.3 M KCl, and 0.5 mM DTT (basic buffer). Previous work showed that this protocol yielded about 90% phosphorylation of the two PKA sites (Robertson et al., 1982).

Labeling of cTnI Mutant. cTnI was first dialyzed against the basic buffer, followed by a second dialysis in which DTT was omitted. The sulfhydryl-reduced protein was reacted with a 3-fold molar excess of IAANS in the presence of 6 M urea at 4 °C for 10 h. The reaction was terminated with a 3−5-fold molar excess of DTT, followed by dialysis against the basic buffer in the presence of 6 M urea to remove unreacted fluorophore. The resulting labeled protein was further dialyzed against the basic buffer in the absence of urea, and this dialysis was repeated twice. The concentration of IAANS-labeled cTnI mutant was determined with either a turbidimetric tannin micromethod (Mejbaum-Katzenellenbogen & Dobryszycha, 1959) or the Bradford method (Bradford, 1976), and the amount of covalently labeled IAANS was determined by absorbance using a molar extinction coefficient of 24 900 M^{-1} cm^{-1} at 325 nm (Johnson et al., 1980). The labeling ratio was >0.9 mol fluorophore/mol of protein.

Steady-State Fluorescence Measurements. Steady-state fluorescence measurements were carried out at 20 ± 0.1 °C on an SLM 8000C spectrofluorometer. The band pass of both the excitation and emission monochromators was set at 3 nm, and the measurements were made in the ratio mode. Emission spectra were corrected for variations of the detector system response with wavelengths. The fluorescence intensity of IAANS attached to a cTnI mutant decreased slowly immediately upon illumination, but approached a limiting level within 90 s. The lost intensity was fully reversible after a brief period in the dark. It was necessary to use a standardized timing to record the intensity. This procedure was found to yield reproducible results.

Quantum yield of IAANS was determined by the comparative method, using quinine sulfate in 0.1 N H_2SO_4 as the standard (0.52 at λ_{ex} = 465 nm and 0.47 at λ_{ex} = 325 nm) (Melhuish, 1964):

$$\frac{Q_p}{Q_{qs}} = \frac{A_{qs}F(\lambda)_p}{A_pF(\lambda)_{qs}} \quad (1)$$

where subscripts p and qs refer to probe (IAANS) and quinine sulfate, respectively, Q is quantum yield, A is probe absorbance at the excitation wavelength, and $F(\lambda)$ is the area of the corrected emission spectrum. Absorption spectra were recorded on a Beckman DU-40 spectrophotometer at room temperature.

Quenching of IAANS fluorescence intensity was measured by adding aliquots of an 8 M acrylamide to the sample. When neccessary, a correction was made for inner filter effects. The emission was measured at 459 nm for nonphosphorylated sample and at 467 nm for phosphorylated samples with excitation at 325 nm. The quenching data were analyzed by either the Stern−Volmer equation

$$\frac{F_o}{F} = 1 + K_{SV}[Q] \quad (2)$$

or a modified Stern−Volmer equation (Lehrer & Leavis, 1978)

$$\frac{F_o}{F_o - F} = \left(\sum \frac{f_iK_{SV,i}[Q]}{1 + K_{SV,i}[Q]}\right)^{-1} \quad (3)$$

where F_o and F are the fluorescence intensities in the absence and presence of quencher, respectively, [Q] is the molar quencher concentration, K_{SV} is the Stern−Volmer dynamic quenching constant. Equation 3 is applicable to multiple classes of emitting species, each with its own fractional intensity f_i and Stern−Volmer constant, $K_{SV,i}$.

Time-Resolved Fluorescence Measurements. Fluorescence intensity decay and anisotropy decay of IAANS linked to mutant cTnI were measured in the basic buffer at 20 °C on a PRA single-photon counting system (model 3000) with a DCM [4-(dicyanomethylene)-2-methyl-6-(*p*-dimethylaminostyryl-4*H*-pyran)] dye laser synchronously pumped by a mode-locked argon ion laser (model 171, Spectra-Physics). The mode-locker operated at 41 MHz, and the cavity-dumped laser was set at 4 MHz and provided a train of light pulses with a 15 ps full width at half-maximum (FWHM). The output from the dye laser was frequency-doubled to 325 nm by an angle-tuned KDP crystal (model 390, Spectra-Physics) to generate uv picosecond laser pulses with tunable frequency from 315 to 335 nm. The laser intensity was attenuated by neutral density filters such that the emitted photon counting rate was reduced to <3 kHz to avoid photon pileup. The PM tube was a Hamamatsu R955, and the photon counting system had a response time of ~500 ps in FWHM.

For lifetime measurements, the excitation polarizer was set at the vertical direction and the emission polarizer was oriented at the magic angle (54.7° from the horizontal). The emission was detected at a right angle to the excitation beam. The emission wavelengths were selected with either a 4-nm band pass monochromator (Instrument SA, Inc.) or a Ditric 3-cavity 334-nm interference filter. Decay curves were collected into 1024 channels of a multichannel analyzer at a resolution of 20−30 ps/channel until 2×10^4 photons were collected in the peak channel. The decay data were fitted to a sum of exponential terms (Grinvald & Steinberg, 1974) by using a least-squares reconvolution procedure:

$$F(t) = \sum \alpha_i \exp(-t/\tau_i) \quad (4)$$

where τ_i are the lifetimes and α_i are the associated fractional amplitudes. The goodness of fit was evaluated by the reduced chi-squares ratio (χ^2_R), the weighted residuals, and the Durbin−Watson parameter (D−W). In the present experiments, $0.9 < \chi^2_R < 1.2$, and D−W > 1.8.

Anisotropy decays were determined by using polarized excitation and measuring the emitted light polarized in the vertical [$F_{||}(t)$] and horizontal [$F_\perp(t)$] directions. Typically, 40 000−50 000 photons were collected in the peak channel for $F_{||}(t)$, and the $F_\perp(t)$ component was counted for the same length of time as for $F_{||}(t)$. The time-dependent anisotropy $r(t)$ was calculated from the difference and sum curves obtained from the two polarized components:

$$F(t) = \frac{F_{||}(t) - GF_\perp(t)}{F_{||}(t) + 2GF_\perp(t)} \quad (5)$$

The G-factor, which corrects for optical differences in the collection of the two polarized decay components, is the ratio of the vertically polarized and horizontally polarized emission intensities obtained with horizontally polarized excitation (Wang et al., 1992). The calculated anisotropy data were fitted to a sum of exponential terms:

$$r(t) = r_o\sum g_i \exp(-t/\phi_i) \quad (6)$$

where ϕ_i are the rotational correlation times with fractional amplitudes g_i, and r_o is the limiting anisotropy at zero time. For a two-component fit, the total anisotropy r_o is given by $r_o = g_1r_o + g_2r_o$, with $g_1 + g_2 = 1$.

Reagents and Chemicals. IAANS was obtained from Molecular Probes (Eugene, OR) and used without further purification. It was dissolved in dimethylformamide at concentrations of 10−15 mM and stored in the dark at either 4 or −20 °C. The catalytic subunit of protein kinase A from beef heart was obtained from Sigma (St. Louis, MO). Taq DNA polymerase was purchased from Promega.

RESULTS

Characterization of Mutant cTnI. To establish that the mutations in cTnI had no detrimental effect on the functional properties of the protein, we tested the ability of mutants to regulate Ca^{2+}-dependent ATPase activity in reconstituted myofibrillar preparations. Wild type and mutant cTnI were complexed with cTnC and reconstituted into myofibrillar preparations in which native cTnI−cTnC complex was extracted by treatment with exogenous cTnT as previously described (Wattanapermpool et al., 1995). In the presence of EGTA (pCa 8.5), ATPase activity of preparations containing mutant cTnI was moderately (12%) higher compared to the wild type cTnI. When tested at pCa 4.8, ATPase activity of preparations containing mutant cTnI was only 2% higher than the wild type cTnI, and this difference was found to be statistically insignificant.

Steady-State Fluorescence of cTnI$_{IAANS}$. The steady-state emission spectrum of mutant cTnI labeled with IAANS at Cys-5 showed a peak at 459 nm. The emission peak was essentially unchanged when the mutant was complexed with

Table 1: Fluorescence Emission Spectral Parameters of Mutant cTnI Labeled with IAANS at Cys-5[a]

sample	quantum yield	emission peak, nm	sample	quantum yield	emission peak, nm
cTnI	0.047	459	p-cTnI	0.010	467
cTnI + cTnC	0.044	458	p-cTnI + cTnC	0.010	466
cTnI + cTnC + Mg^{2+}	0.033	456	p-cTnI + cTnC + Mg^{2+}	0.009	466
cTnI + cTnC + Mg^{2+} + Ca^{2+}	0.039	460	p-cTnI + cTnC + Mg^{2+} + Ca^{2+}	0.011	464

[a] cTnI denotes mutant cTnI labeled with IAANS at Cys-5 and cTnC denotes native cTnC. When cTnC was present, labeled cTnI was incubated with a 2−3-fold stoichiometric excess of cTnC for several hours before measurements were taken. See Figure 1 for other conditions.

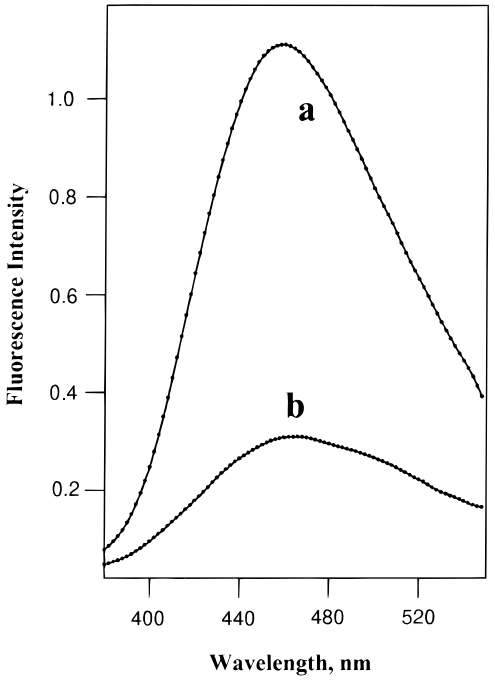

FIGURE 1: Fluorescence emission spectra of mutant cTnI(S5C/C81I/C98S) labeled with IAANS at Cys-5. (a) Unphosphorylated mutant and (b) phosphorylated mutant. Protein concentration was 2 μM in 30 mM MOPS at pH 7.0, 1 mM EGTA, 0.3 M KCl, and 0.5 mM DTT. Samples were excited at 325 nm, 20 °C. The spectral parameters are given in Table 1.

apo cTnC, but the intensity decreased slightly (~6%). The presence of Mg^{2+} resulted in a further decrease of the quantum yield (~30%) of the labeled mutant cTnI in the binary protein complex. Subsequent addition of Ca^{2+} recovered about 17% of the lost intensity. The emission spectrum of the binary complex was slightly blue-shifted in the presence of Mg^{2+}, and the addition of Ca^{2+} resulted in a red-shift of the spectrum. These results are summarized in Table 1.

The intensity of phosphorylated cTnI mutant was considerably lower than the corresponding unphosphorylated protein (Figure 1), and the quantum yield was reduced by a factor of 4−5. Relative to the unphosphorylated mutant, the emission spectrum of the PKA phosphorylated mutant displayed a 8-nm red-shift in the λ_{max} from 459 to 467 nm. These spectral properties were only slightly affected when the phosphorylated protein was complexed with apo cTnC or with cTnC in the presence of Mg^{2+}. A small blue-shift of the spectrum was observed in the presence of Ca^{2+}. This Ca^{2+} effect, although small, was in the opposite direction of that observed with unphosphorylated mutant cTnI complexed with cTnC.

Fluorescence Intensity Decay of Mutant cTnI Labeled with IAANS. The intensity decay of IAANS-labeled mutant cTnI was analyzed by a sum of exponential terms. The data could not be fitted to either a monoexponential function or a biexponential function, but the fit was considerably improved with a triexponential function (Figure 2). The recovered three lifetimes were well separated, and the two longer components contributed over 85% to the total emission (Table 2). The intensity decay profiles of the protein complexed with cTnC, both in the absence of added cation or in the presence of Mg^{2+} and Ca^{2+}, were very similar to that shown in Figure 2. The decay parameters recovered for the complex in different ionic conditions are summarized in Table 2. The three lifetimes were well separated in every case and appeared not be sensitive to cations.

As shown in Figure 3, the intensity decay curve of phosphorylated mutant cTnI labeled with IAANS had a shape very different from that observed with unphosphorylated cTnI mutant. The data could not be fitted with a triexponential function and required a fourth exponential term for a satisfactory fit. As in the case of unphosphorylated mutant cTnI, the recovered lifetimes were well separated, with the ratio of any two lifetimes >2. It is noted that the excitation light source used in the present study was a synchronously pumped dye laser with very narrow pulse widths, and the detector system had a sub-nanosecond response. These instrumental responses and the large difference in the ratio of τ_i/τ_{i+1} provided assurance that the decay model we chose was reasonable. The decay parameters for the phosphorylated cTnI mutant and its complex with cTnC are also summarized in Table 2.

The additional decay component of the phosphorylated cTnI mutant had a long lifetime (7.2−8.6 ns). In spite of the presence of this longer component, the weighted mean lifetime of the phosphorylated protein was shorter than the unphosphorylated protein. This decrease was due to the fact that the shortest component now became the dominant species, contributing 30% to the total emission intensity. Becasue of incomplete and possible heterogeneous phosphorylation of the PKA sites, it was unclear how each of the three decay components of the unphosphorylated protein was affected by the phosphorylation. The differences in mean lifetimes between the unphosphorylated and phosphorylated protein were consistent with the differences in quantum yields and spectral peaks between the two forms of the protein. Qualitatively, the phosphorylation resulted in changes in both the steady-state and decay properties of the IAANS probe in the same direction.

Anisotropy Decay of Mutant cTnI$_{IAANS}$. Figure 4 is a representative anisotropy decay curve of mutant cTnI labeled at Cys-5 with IAANS. The decay was biexponential, characterized by two rotational correlation times. The biexponential characteristic of the decay was retained regardless of the state of phosphorylation of the mutant, whether the protein was complexed with cTnC, and ionic conditions. The anisotropy decay parameters obtained under these different conditions are given in Table 3. The long correlation time of unphosphorylated cTnI increased by 3 ns from

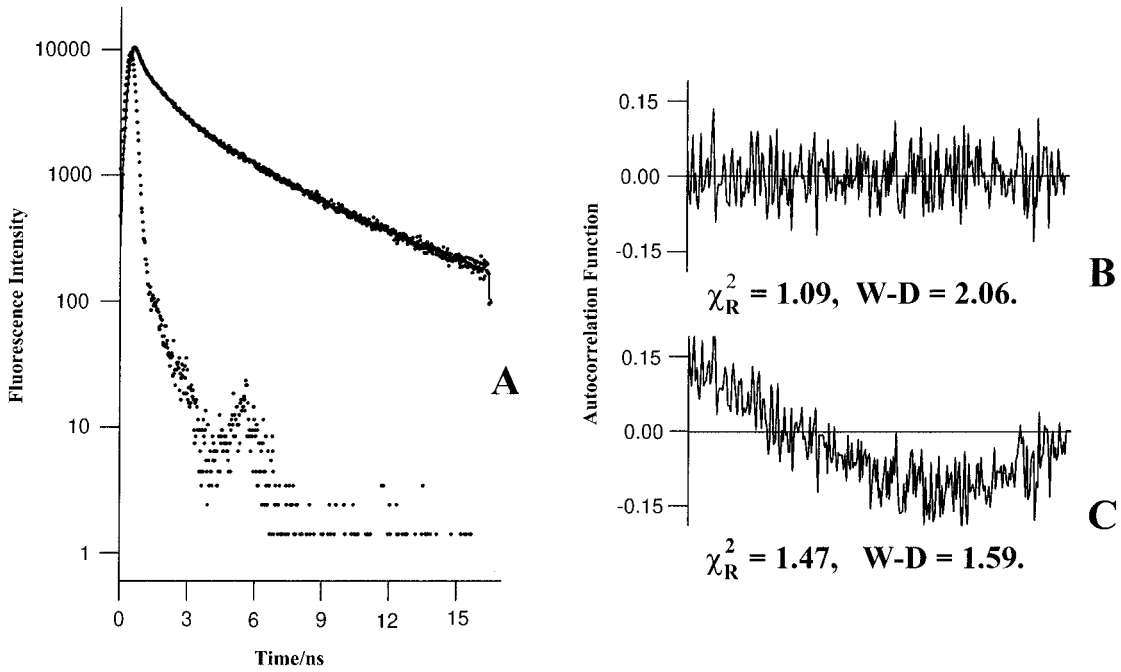

FIGURE 2: Fluorescence intensity decay of IAANS attached to Cys-5 of unphosphorylated cTnI mutant. (A) The intensity decay was fitted to a triexponential function (solid curve). The sharp peak on the left shows the laser profile. This fit yielded the following parameters: $\tau_1 = 4.81$ ns, $\tau_2 = 1.15$ ns, $\tau_3 = 0.096$ ns, $\alpha_1 = 0.0.08$, $\alpha_2 = 0.0.14$, $\alpha_3 = 0.0.79$; $\chi_R^2 = 1.09$ and D−W = 2.06. (B) Autocorrelation function of the residuals for the fit shown in A. (C) Autocorrelation function of the residuals for a biexponential fit of the same set of data shown in A. This nonrandom autocorrelation function indicates that the fit was unacceptable. For this unacceptable biexponential fit, $\chi_R^2 = 1.47$ and W−D = 1.59. Protein concentration was 2 μM, λ_{ex} was 325 nm, and λ_{em} was 450 nm. See the legend for Figure 1 for other conditions.

Table 2: Fluorescence Intensity Decays of Mutant cTnI Labeled with IAANS at Cys-5[a]

sample	τ_i (ns)	α_i	f_i	$<\tau>$ (ns)	χ_R^2	D−W
cTnI	4.81 ± 0.05	0.08 ± 0.01	0.62	3.27	1.09	2.22
	1.15 ± 0.02	0.14 ± 0.01	0.26			
	0.096 ± 0.010	0.79 ± 0.03	0.13			
cTnI + cTnC	4.83 ± 0.04	0.10 ± 0.01	0.65	3.42	1.13	2.04
	1.18 ± 0.03	0.17 ± 0.01	0.26			
	0.10 ± 0.01	0.72 ± 0.03	0.09			
cTnI + cTnC + Mg^{2+}	4.78 ± 0.06	0.16 ± 0.01	0.66	3.48	1.11	2.17
	1.14 ± 0.02	0.28 ± 0.03	0.28			
	0.13 ± 0.01	0.56 ± 0.04	0.06			
cTnI + cTnC + Mg^{2+} + Ca^{2+}	4.84 ± 0.06	0.15 ± 0.01	0.66	3.52	1.13	2.13
	1.15 ± 0.02	0.26 ± 0.19	0.27			
	0.14 ± 0.01	0.59 ± 0.03	0.07			
p-cTnI	8.36 ± 0.09	0.005 ± 0.001	0.16	2.58	1.14	1.96
	3.00 ± 0.02	0.029 ± 0.005	0.33			
	0.82 ± 0.01	0.068 ± 0.009	0.21			
	0.090 ± 0.010	0.890 ± 0.053	0.30			
p-cTnI + cTnC	7.21 ± 0.08	0.012 ± 0.008	0.25	2.89	1.06	1.00
	2.80 ± 0.03	0.04 ± 0.01	0.32			
	0.82 ± 0.02	0.091 ± 0.023	0.22			
	0.087±0.01	0.86 ± 0.062	0.22			
p-cTnI + cTnC+ Mg^{2+}	7.66 ± 0.09	0.009 ± 0.001	0.21	2.75	1.06	2.17
	2.77 ± 0.03	0.039 ± 0.009	0.34			
	0.76 ± 0.02	0.085 ± 0.012	0.20			
	0.092 ± 0.010	0.87 ± 0.04	0.25			
p-cTnI + cTnC + Mg^{2+} + Ca^{2+}	7.57 ± 0.08	0.015 ± 0.030	0.29	2.93	1.07	1.99
	2.73 ± 0.03	0.08 ± 0.01	0.37			
	0.74 ± 0.03	0.16 ± 0.02	0.20			
	0.11 ± 0.02	0.81 ± 0.04	0.14			

[a] cTnI denotes mutant cTnI labeled at Cys-5 with IAANS, and cTnC refers to native cTnC. p-cTnI is phosphorylated mutant cTnI labeled with IAANS. τ_i are the lifetimes of the attached IAANS, α_i are the associated fractional amplitudes, f_i are the fractional intensities calculated from $f_i = \alpha_i\tau_i/\sum\alpha_i\tau_i$, and $<\tau>$ is the intensity-weighted mean lifetime calculated from $<\tau> = \sum\alpha_i\tau_i^2/\sum\alpha_i\tau_i$. The uncertainties in τ_i and α_i are the standard errors obtained from the nonlinear least-squares fitting. cTnI concentration was ~2 μM. Other conditions were the same as given in Table 2.

13.6 to 16.7 ns upon complexation with cTnC, and this correlation time of the binary protein complex further increased in the presence of Mg^{2+} and Mg^{2+} plus Ca^{2+}. This long correlation time reflected the overall global motion of the mutant or its binary complex with cTnC. The 1−2 ns increase in the global correlation time observed in the presence of cations suggested a more asymmetric hydrodynamic shape of the binary protein complex induced by cation binding to cTnC. The short correlation times, which were in the sub-nanosecond regime, suggested considerable mobility of the attached fluorescent probe. The angular range of the rotational mode of the short correlation time was

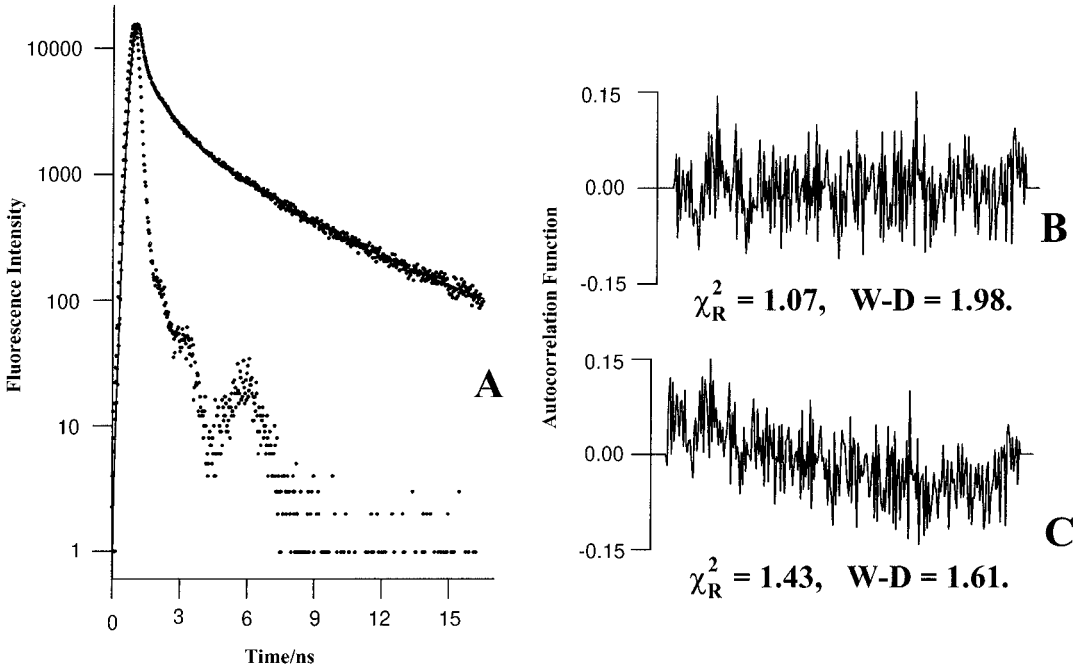

FIGURE 3: Fluorescence intensity decay of IAANS attached to Cys-5 of the phosphorylated cTnI mutant. Conditions were the same as for results shown in Figure 2. (A) Laser profile as the sharp peak and the decay data fitted to four exponential terms (solid curve). (B) Autocorrelation function of the residuals for the fit shown in A. (C) Autocorrelation function of the residuals for a triexponential fit of the same set of data. The best-fitted parameters from A are listed in Table 2.

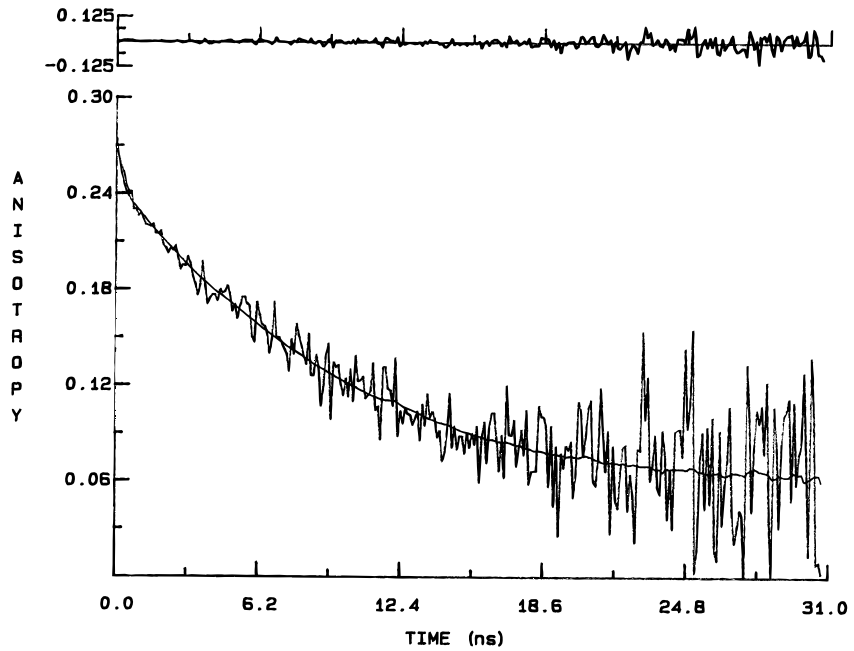

FIGURE 4: Representative plot of the fluorescence anisotropy decay of IAANS attached to Cys-5 of unphosphorylated cTnI mutant. The data were fitted to a biexponential function, yielding two rotational correlation times: $\phi_1 = 0.14$ ns and $\phi_2 = 13.60$ ns, $\chi^2_R = 1.16$ and D−W = 2.02. The panel across the top of the figure is the autocorrelation function of the residuals of the fit. Experimental conditions were the same as those given in Figure 1.

expressed as a cone semiangle (θ). The magnitude of θ reflected the angular amplitude of the motion of the attached probe. Phosphorylation resulted in a decrease of the long correlation time from 13.6 to 9.23 ns, whereas the short correlation time was only slightly affected. This phosphorylation-induced decrease in the long correlation time was carried over to the binary complex with cTnC. The limiting anisotropy (r_o) of IAANS linked to Cys-5 in the unphosphorylated cTnI mutant was in the range 0.272−0.296 and was not affected by complexation with cTnC or different ionic conditions. This parameter, however, was substantially larger for the phosphorylated mutant (0.309−0.329). The values of θ determined with the phosphorylated cTnI were 3−4° smaller than with the unphosphorylated cTnI mutant.

Fluorescence Quenching by Acrylamide. The accessibility of IAANS linked to Cys-5 of mutant cTnI to solvent was determined before and after phosphorylation, using acrylamide as the quenching agent. The Stern−Volmer quenching plots for unphosphorylated mutant are shown in Figure 5. These plots were essentially linear, with Stern−Volmer constants (K_{SV}) in the range of 1.6−1.8 M^{-1} and bimolecular quenching constants k_q in the range of (4.5−5.5) × 10^8 M^{-1} s^{-1}. For comparison, the quenching properties of IAANS covalently linked to 2-mercaptoethanol dissolved in a 1:10

Table 3: Anisotropy Decays of IAANS-Labeled cTnI Mutant and Its Complex with cTnC[a]

sample	ϕ_i (ns)	$g_i r_o$	r_o	θ (deg)	χ^2_R	D−W
cTnI	0.14	0.060	0.287	22.4	1.16	2.02
	13.6	0.227				
cTnI + cTnC	0.243	0.065	0.296	23.1	1.19	1.98
	16.7	0.231				
cTnI + cTnC + Mg^{2+}	0.197	0.047	0.272	20.2	1.11	2.05
	17.9	0.225				
cTnI + cTnC + Mg^{2+} + Ca^{2+}	0.16	0.057	0.277	22.2	1.19	1.88
	18.6	0.220				
p-cTnI	0.17	0.050	0.310	19.5	1.20	1.90
	9.23					
p-cTnI + cTnC	0.19	0.048	0.329	18.6	1.17	1.89
	12.3					
p-cTnI + cTnC + Mg^{2+}	0.16	0.047	0.313	18.7	1.15	1.98
	13.7	0.266				
p-cTnI + cTnC + Mg^{2+} + Ca^{2+}	0.83	0.051	0.309	19.7	1.11	1.87
	14.8	0.258				

[a] cTnI denotes mutant cTnI labeled with IAANS at Cys-5, and cTnC is native cardiac TnC. ϕ_i are the rotational correlation times with associated anisotropies $g_i r_o$. $r_o = g_1 r_o + g_2 r_o$ is the limiting anisotropy at zero time. θ is the cone semiangle over which the fluorophore moves and was calculated from the amplitudes of the two rotational modes from $g_2 r_o/(g_1 r_o + g_2 r_o) = (1/4)\cos^2\theta(1 + \cos\theta)^2$. The standard errors were in the range 0.03−0.05 ns for ϕ_1 (short component) and (0.15−0.32) ns for ϕ_2 (long component) for all samples. The standard errors for $g_1 r_o$ were 0.002−0.007 and for $g_2 r_o$ were 0.003−0.008.

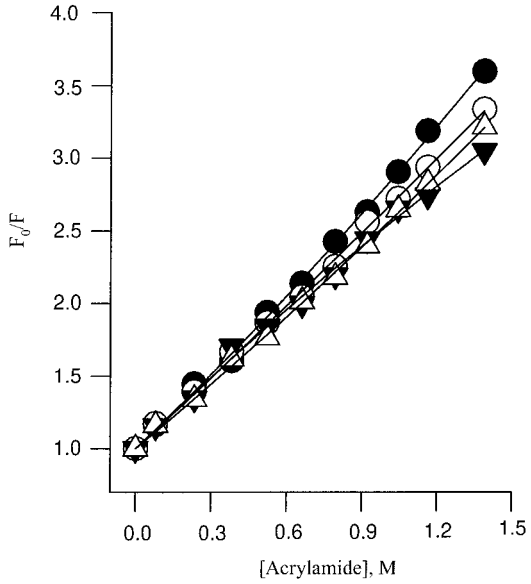

FIGURE 5: Stern−Volmer plots for the quenching of the steady-state fluorescence of IAANS attached to Cys-5 of the unphosphorylated cTnI mutant. Closed circle, cTnI alone; open circle, cTnI complexed with cTnC; closed triangle, cTnI complexed with cTnC + Mg^{2+}; open triangle, cTnI complexed with cTnC + Mg^{2+} + Ca^{2+}. F_o is the intensity in the absence of acrylamide and F is the intensity in the presence of acrylamide. Protein concentration was 2 μM. Other conditions were the same as those given for Figure 1.

(v/v) ethanol/water mixed solvent were measured (data not shown). The K_{SV} for this system was 0.20 M^{-1} and k_q was 6.38×10^8 M^{-1} s^{-1}. These results suggested that IAANS attached to Cys-5 was highly accessible to collision with solvent. This accessibility was not affected in the complex with cTnC, in the absence or presence of cations. The quenching parameters are listed in Table 4.

Very different quenching patterns were observed with the phosphorylated cTnI mutant. The Stern−Volmer plots displayed downward curvatures (Figure 6). In 1.4 M acrylamide, about 50−60% of the intensities of the phosphorylated cTnI were quenched, whereas about 70% of the intensities of the unphosphorylated cTnI were quenched (Figure 5). The downward curvatures suggested additional decay components of the attached IAANS when compared with the unphosphorylated cTnI. The concave downward Stern−Volmer plots were fitted to eq 3 with two exponential terms. Two Stern−Volmer constants were recovered, one being larger than 2 M^{-1} and the other being smaller than 1 M^{-1}. To simplify the two-component analysis, one Stern−Volmer constant was initially constrained at a value close to the single K_{SV} value determined with the unphosphorylated mutant. The recovered second Stern−Volmer constant was 2−3-fold smaller than the value from the unphosphorylated protein, but had a significant fractional amplitude (∼75%). These parameters are summarized in Table 4. The two Stern−Volmer constants could be attributed to two populations of labeled cTnI: (a) a small population consisting of unphosphorylated protein or protein with a very low degree of phosphorylation and (b) a large population consisting of phosphorylated cTnI with Stern−Volmer constants in the range of 0.5−0.8 M^{-1}, a factor of 2−3-fold smaller than that for the unphosphorylated species. Regardless of the composition of the phosphorylated population, the recovered small Stern−Volmer constant was a composite value, reflecting the behavior of the various phosphorylated species. The observed value of the bimolecular quenching constant (k_q) was also a composite value with contributions from all cTnI species. It was not possible to separate the contribution of the unphosphorylated species from those of the phosphorylated species because the mean lifetimes of the species was used to calculate k_q. Qualitatively, what emerged from these quenching results is that the phosphorylation resulted in considerable shielding of the IAANS labeled at Cys-5 from collisional quenching.

DISCUSSION

There is ample evidence that the phosphorylation of cTnI at its amino terminus is an important determinant of the affinity of cTnC for Ca^{2+} and thus the dynamics of cardiac relaxation and contraction (Solaro, 1993). Yet the molecular basis by which phosphorylation of cTnI modulates cardiac muscle contractility is obscure. Structural changes induced by phosphorylation may ultimately modulate cardiac function by changing the affinity of cTnI for cTnC, cTnT, or actin. A phosphorylation-induced decrease in the apparent affinity of cTnI for cTnC has been reported (Liao et al., 1994). We have tested the hypothesis that phosphorylation of Ser-23

Table 4: Quenching Parameters of the Fluorescence of IAANS-Labeled Mutant cTnI[a]

sample	quenched intensity	K_{SV} M^{-1}	$k_q \times 10^{-8}$ M^{-1} s^{-1}	sample	quenched intensity	K_{SV} M^{-1}	f_i	$k_q \times 10^{-8}$ M^{-1} s^{-1}
cTnI	0.72	1.83	5.6	p-cTnI	0.49	1.96	0.25	2.91
						0.49	0.75	
cTnI + cTnC	0.70	1.68	4.9	p-cTnI + cTnC	0.57	1.78	0.27	2.84
						0.65	0.73	
cTnI + cTnC + Mg^{2+}	0.67	1.78	5.1	p-cTnI + cTnC + Mg^{2+}	0.52	1.89	0.29	2.70
						0.58	0.71	
cTnI + cTnC + Mg^{2+} + Ca^{2+}	0.69	1.58	4.5	p-cTnI + cTnC + Mg^{2+} + Ca^{2+}	0.59	1.70	0.29	2.44
						0.83	0.71	

[a] cTnI denotes mutant cTnI labeled at Cys-5 with IAANS, p-cTnI is phosphorylated cTnI, and cTnC is native cardiac TnC. The quenched intensity was the intensity determined at 1.4 M acrylamide and normalized to the intensity determined in the absence of quencher. K_{SV} is the Stern−Volmer dynamic quenching constant, and k_q is the bimolecular quenching rate constant calculated from $k_q = K_{SV}/\langle\tau\rangle$. For phosphorylated samples, the Stern−Volmer constant was resolved into two components with fractional amplitude f_i. The mean value of the two resolved K_{SV} values was used to calculate k_q for the phosphorylated samples.

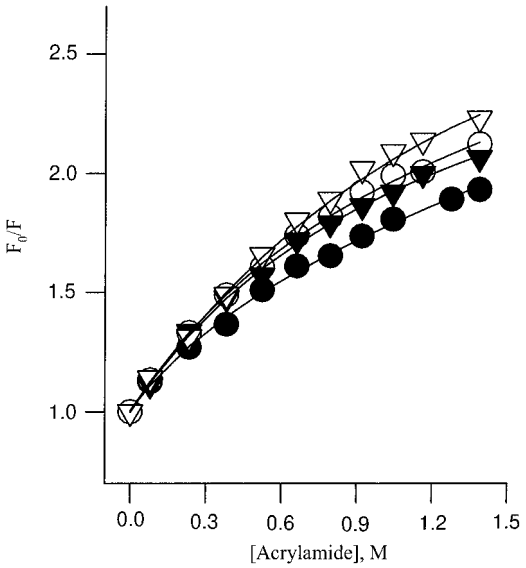

FIGURE 6: Stern−Volmer plots for the quenching of the steady-state fluorescence of the phosphorylated cTnI mutant labeled at Cys-5 with IAANS. Closed circle, cTnI alone; open circle, cTnI + cTnC; closed triangle, cTnI + cTnC + Mg^{2+}; and open triangle, cTnI + cTnC + Mg^{2+} + Ca^{2+}. F_o and F are the intensities in the absence and presence of acrylamide, respectively. Conditions were the same as given in Figure 5.

and Ser-24 has a structural effect on the N-terminal extension as well as on the overall conformation of the protein. Our approach involved the generation of a single-cysteine mutant cTnI(S5C/C81I/C98S) for probing the local conformation of the N-terminal extension using the fluorescent probe IAANS covalently linked to Cys-5. The spectral results provide evidence that the conformation of the N-terminal extension of cardiac cTnI is profoundly affected by phosphorylation.

The structure of the N-terminal extension of cTnI is not known, but this segment is unlikely to have a well-defined secondary structure (Liao et al., 1992). IAANS attached to a side chain near the N-terminus within this segment is likely very accessible to solvent. The emission peak of the unphosphorylated labeled mutant is consistent with this idea. Moreover, the bimolecular quenching constant indicates that the attached probe is highly accessible to collisional quenching. A previous study of the fluorescence anisotropy decay of Trp-192 in native cTnI showed that phosphorylation resulted in a 38% decrease in the long correlation time (Liao et al., 1992). This decrease is corroborated in the present study (33% decrease in the long correlation time), using an extrinsic probe located at the opposite end of the elongated protein, although the values of the correlation time determined by the two different fluorophores are different. The value of rotational correlation times calculated from anisotropy decay data are dependent upon the average orientations of transition dipoles with respect to the principal rotational diffusion axis of the protein (Harvey & Cheung, 1977; Barkley et al., 1981). These orientations of Trp-192 in native cTnI and IAANS attached to Cys-5 in mutant cTnI are not known, but it is highly unlikely that they are very similar. Because of the likely difference in dipole orientations, the different correlation times sensed by the different probes are not unexpected. The important finding is that both probes, one located near the C-terminus and the other located near the N-terminus, sense a very similar phosphorylation-induced reduction of the long correlation time. This decrease is probe-independent and not affected by probe location. As discussed previously (Liao et al., 1992), a simple explanation of the decreased correlation time is a decrease in the apparent axial ratio of the phosphorylated cTnI mutant when compared with the unphosphorylated mutant. In addition to the influence of dipole orientations of the fluorophore, the measured long correlation time always is a lower limit of the global correlation time of the molecule. This arises from internal motions of the fluorophore about certain axes, and this leads to a depolarization effect. The IAANS probe attached to Cys-5 has considerable mobility as reflected by the observed limiting anisotropy of 0.287. Phosphorylation increases r_o to 0.310, a value approaching that of free IAANS measured in a high-viscosity medium at a low temperature. This increase in r_o is accompanied by a decrease of the cone semiangle. These two results provide evidence that the attached IAANS has less flexibility in phosphorylated cTnI than in the nonphosphorylated protein, and this more restricted internal motion is expected to result in a longer measured correlation time. The observed phosphorylation effect, however, is in the opposite direction: a shorter correlation time. Thus, the observed shorter correlation time must be due to changes in the conformation of cTnI. These changes are interpreted in terms of a change of the hydrodynamic shape of the protein and suggest a folding of the N-terminal extension.

Folding of the N-terminal extension of cTnI may be due to electrostatic interactions. The N-terminal extension of cTnI has four arginines at positions 20, 21, 22, and 28. The segment from residues 20 to 28 is likely extended at neutral pH because of electrostatic repulsion. The two phosphorylation sites (Ser-23 and Ser-24) are located within this cluster of basic residues. Phosphorylation introduces negatives charges within this cluster of arginyl side chains and can

lead to a collapse of the extended segment and a partial folding of the segment due to electrostatic interactions. ^{31}P-NMR studies of synthetic peptides with sequences corresponding to residues 18−27 indicated that phosphoserine at position 24 was near to one of the three contiguous arginyl residues, strongly suggesting interaction between the phosphate group and one of the arginine side chains (Jaquet et al., 1993). This putative interaction is consistent with the present suggestion of a folding of the N-terminal segment in the the phosphorylated cTnI mutant. Ser-23 and Ser-24 can be phosphorylated in the binary complex formed with cTnC and in troponin. It has been recently reported that bisphosphorylated cTnI was readily dephosphorylated, but could not be dephosphorylated when the cTnI was complexed with cTnC (Al-Hillawi et al., 1995). The latter information indicates that the phosphate groups in the binary complex are not accessible and suggests phosphorylation-induced contacts between the N-terminal extension of cTnI and cTnC. The short sequence containing several prolines immediately adjacent to the N-terminal end of the three arginines could provide a fairly rigid structure and act as a "spacer" arm enabling the N-terminal extension to fold and part of the N-terminal extension to become an additional site for cTnC (Al-Hillawi et al., 1995). The present spectroscopic data are compatible with these ideas.

Since IAANS is an environmentally sensitive probe, changes of its emission properties such as those observed with the phosphorylated cTnI (i.e., decreases in quantum yield and lifetime and red spectral shift) are usually indicative of an environment that has become more exposed to solvent (Lippert, 1957). An increased exposure of the attached IAANS induced by phosphorylation is in apparent conflict with the observed decrease in collisonal quenching. Interaction of the excited-state fluorophore with aqueous solvent generally results in solvent relaxation and reduction of radiative rates, thus leading to a red spectral shift, decreased quantum yield, and shorter lifetimes. These spectral changes result from the dielectric constant and refractive index (Lippert, 1957). Interaction of the same fluorophore in a protein with neighboring side chains can also lead to similar changes in emission properties (Dong & Cheung, 1996). A partial folding of the N-terminal extension may bring the fluorescent probe attached to Cys-5 to a close proximity of other residues. If ground-state interactions between IAANS and the side chains of these residues occur, even if only transiently, the emission of the probe is expected to be quenched. This quenching can be very substantial. The observed fluorescence properties of IAANS in the phosphorylated cTnI mutant reflect a balance of this internal quenching and changes of the conformation of the peptide segment that may lead to a shielding of the probe from collisional quenching. The internal quenching brought about by the folding appears to play a dominant role in determining the overall emission properties. The putative ground-state interactions may involve residues far away from the N-terminus in the linear sequence, dependent upon the nature of the folded conformation. The present data do not provide information on this.

In summary, the results from several types of fluorescence measurements on a cTnI mutant show that phosphorylation of the N-terminal extension leads to substantial changes in the conformation of the N-terminal extension and a more compact hydrodynamic shape of the protein. These results are compatible with a phosphorylation-induced folding of the N-terminal segment. In the following paper (Dong et al., 1997), we will present a fluorescence resonance energy transfer study that supports this suggestion.

REFERENCES

Al-Hillawi, E., Bhandar, D. G., Trayer, H, R., & Trayler, I. P (1995) *Eur. J. Biochem. 228*, 962−970.

Allen, D. G., & Kurihara, S. (1980) *Eur. Heart J. 1*, 5−15.

Barkley, M. D., Kowalczyk, A. L., & Brand, L. (1981) *J. Chem. Phys. 75*, 3581−3589.

Bradford, M. D. (1976) *Anal. Biochem. 71*, 248−254.

Dong, W.-J., & Cheung, H. C. (1996) *Biochim. Biophys. Acta 1295*, 139−146.

Dong, W.-J., Chandra, M., Xing, J., She, M., Solaro, R. J., & Cheung, H. C. (1997) *Biochemistry 36*, 6754−6761.

Grinvald, A., & Steinberg, I. Z. (1974) *Anal. Biochem. 59*, 583−589.

Guo, X., Wattanapermpool, J., Palmiter, K. A., Murphy, A. M., & Solaro, R. J. (1994) *J. Biol. Chem. 269*, 15210−15216.

Harvey, S. C., & Cheung, H. C. (1977) *Biochemistry 16*, 5181−5187.

Herig, J. W., Kohler, G., Pfitzer, G., Rüegg, J. C., & Wilffle, G. (1981) *Pflugers Arch. Eur. J. Physiol. 391*, 208−212.

Ho, S. N., Hunt, H. D., Horton, R. M., Pullern, J. K., & Pease, L. R. (1989) *Gene 77*, 51−59.

Jaquet, K., Korte, K., Schnackerz, K., & Hielmeyer, L. M. G. (1993) *Biochemistry 32*, 13873−13878.

Johnson, J. D., Collins, J. H., Robertson, S. P., & Potter, J. D. (1980) *J. Biol. Chem. 255*, 9635−9640.

Lehrer, S. S., & Leavis, P. C. (1978) *Methods Enzymol 49*, 222−236.

Liao, R., Wang, C.-K., & Cheung, H. C. (1992) *Biophys. J. 63*, 986−995.

Liao, R., Wang, C.-K., & Cheung, H. C. (1994) *Biochemistry 33*, 12729−12734.

Lippert, E. (1957) *Z. Elektrochem. 61*, 962−975.

Mejbaum-Katzenellenbogen, W., & Dobryszycha, W. M. (1959) *Clin. Chim. Acta 4*, 515−520.

Melhuish, W. H. (1964) *J. Opt. Soc. Am. 54*, 183−194.

Moir, A. J. G., Solaro, R. J., & Perry, S. V. (1980) *Biochem. J. 185*, 505−513.

Potter, J. D. (1982) *Methods Enzymol. 85*, 241−263.

Robertson, S. P., Johnson, J. D., Holroyde, M. J., Kranias, E. G., Potter, J. D., & Solaro, R. J. (1982) *J. Biol. Chem. 257*, 260−263.

Solaro, R. J. (1986) in *Protein Phosphorylation in the Heart Muscle* (Solaro, R. J., Ed.) pp 129−156, CRC Press Inc., Boca Raton, FL.

Solaro, R. J. (1993) in *Modulation of Cardiac Calcium Sensitivity* (Allen, D. A. G., & Lee, J. A., Eds.) pp 160−177, Oxford University Press.

Solaro, R. J., Moir, A. J. G., & Perry, S. V. (1976) *Nature 262*, 615−617.

Solaro, R. J., Robertson, S. P., Johnson, J. D., Holroyde, M. J., & Potter, J. D. (1981) *Cold Spring Harbor Conf. Cell Proliferation 8*, 901−911.

Swiderek, K., Jaquet, K., Meyer, H. E., & Heilmeyer, L. M. G., Jr. (1988) *Eur. J. Biochem. 176*, 335−342.

Tao, T. Gong, B.-J., & Leavis, P. C. (1990) *Science 247*, 1339−1341.

Wang, C.-K., Mani, R. S., Kay, C. M., & Cheung, H. C. (1992) *Biochemistry 31*, 4289−4295.

Wattanapermpool, J., Guo, X., & Solaro, R. J. (1995) *J. Mol. Cell Cardiol. 27*, 1383−1391.

Zot, A. S., & Potter, J. D. (1987) *Annu. Rev. Biophys. Chem. 16*, 535−559.

BI962226D